

# Distributed Diagnosis of Electric Aircraft Powertrain

Chetan S. Kulkarni, Indranil Roychoudhury, and George Gorospe, Jr

*SGT, Inc., NASA Ames Research Center, Moffett Field, CA, 94035, USA*

*chetan.s.kulkarni@nasa.gov*

*indranil.roychoudhury@nasa.gov*

*george.e.gorospe@nasa.gov*

## ABSTRACT

Electrically powered autonomous aircraft are being increasingly considered for intra-city short-haul air-taxi services to fly human passengers between different locations. As a result, it is critical to incorporate safety under autonomous operations into system operations by enabling such autonomous aircraft to make accurate estimates of its current health state and take the right decisions to complete its mission successfully. The first step to assess health state of the entire aircraft is for the aircraft to be able to assess the health of its individual critical systems, (e.g electrical powertrain) for it to be able to fly and reach its destination in a safe manner. The fundamental components of a powertrain in an electrically powered aircraft include key electrical components such as batteries, motors, and power electronics (e.g., electronic speed controllers). A model-based diagnosis approach of complex critical systems enables their safe and efficient operation. Typically, such model-based schemes are centralized approaches that suffer from inherent disadvantages such as computational complexity, single point of failure, and scalability issues. Distributing the diagnosis task addresses these issues. To this end, this paper presents the results of implementing a distributed diagnostics approach to a representative electric aircraft powertrain. In particular, we focus on the implementation of a distributed diagnosis framework to a quadrotor vehicle. The simulation experiments demonstrate how the distributed diagnosis algorithm correctly and efficiently diagnose faults in the rotorcraft's electric powertrain, such as motor winding faults and electronic speed controller switching faults.

## 1. INTRODUCTION

With improvement in battery technology, progress in developing a practical electric passenger aircraft to be used for intra-city short-haul air-taxi services has steadily accelerated.

Chetan S. Kulkarni et al. This is an open-access article distributed under the terms of the Creative Commons Attribution 3.0 United States License, which permits unrestricted use, distribution, and reproduction in any medium, provided the original author and source are credited.

The trend is inclined more towards using vertical-takeoff-and-landing multirotor aircraft (VTOL) or very-short-takeoff-and-landing (VSTOL) aircraft operated in a fully- or semi-autonomous mode. This inclusion of autonomy raises the critical need for incorporating safety under autonomous operations into system operations. An autonomous electric vehicle should be able to make accurate estimates of its current health state and take the right decisions to complete its mission successfully. This requires assessing the health state of its critical systems, such as its electrical propulsion system, for it to be able to reach its destination in a safe and successful manner.

Electric propulsion systems for aircraft require reliability, resilience, and high power density. These systems must also manage weight, complexity, and operational costs. As more aircraft transition to electric propulsion systems, the management of faults and component degradation becomes increasingly important. Model-based diagnosis of complex critical systems enables their safe and efficient operation. Typically, such model-based schemes are centralized approaches that suffer from inherent disadvantages such as computational complexity, single point of failure, and scalability issues. Distributing the diagnosis task within the overall system framework addresses these issues. To this end, this paper presents the results of applying an online fault diagnosis framework for an electric unmanned aerial systems (e-UAS). In this work we demonstrate the efficacy of the distributed diagnosis framework in detecting and isolating single, persistent, and abrupt faults in electric aircraft powertrain, such as motor winding faults and electronic speed controller switching faults.

In earlier work, an approach for performing system-level prognostics on electrical powertrains (G. Gorospe, Kulkarni, & Hogge, 2017; G. E. Gorospe & Kulkarni, 2017) is being presented. However, in order to perform system-level prognostics on these electric powertrains, the first step is to identify which individual subsystem has failed. As mentioned earlier, in this paper, we implement a distributed diagnosis approach to detect and diagnose the powertrain that has failed.

The result of the fault diagnosis approach forms the foundation for implementing the system-level prognostics framework developed in (Roychoudhury, Biswas, & Koutsoukos, 2010). In this paper, we focus on the distributed diagnosis of a quadrotor aircraft as the current trend in the industry implies multirotor aircraft with VTOL capabilities will be the prime candidates to serve as air-taxis. The modern rotor-crafts usually have four, six, or eight propellers and each has its own powertrain. The distributed fault diagnostic approach presented in this paper can isolate the exact subsystem of one of the multiple powertrains in a computationally efficient manner.

The rest of the paper is organized as follows. Section 2 outlines motivation and background for this work. In Section 3 details of electric powertrain of a quadcopter is discussed. Details of the components developed in the simulation are discussed. Section 4 describes the distributed diagnosis approach implemented in this work. This is followed by Section 5 which covers the experimental setup and results. Conclusions and future work are discussed in Section 6.

## 2. MOTIVATION AND BACKGROUND

The fundamental components of a powertrain in an electrically powered rotorcraft is essentially the same as that of a fixed-wing aircraft. These include key electrical components such as batteries, motors, and power electronics such as electronic speed controllers (ESCs). The motivation for this work evolved from flight operations with the all-electric Edge 540T UAV (Hogge et al., 2018), where during test flights abnormally high current draw was observed from one of the batteries. This caused a critical temperature increase in the motor windings. The developed prognostics algorithm was able to estimate changes in the current drawn by the batteries but this led to investigation into other systems of the power train to identify faults. Investigation of the flight data and troubleshooting with batteries and other hardware confirmed that one of the ESCs on the UAV had degraded since the vehicle was commissioned, and on delving deeper, we identified two switching faults in the ESCs that could occur during operation leading to degradation of the UAS performance. In addition, motor winding faults were also identified to affect UAS performance.

The research presented in (Kulkarni, Celaya, Biswas, & Goebel, 2012; Daigle, Sankararaman, & Kulkarni, 2015) focused on isolated components where component-level prognostics methodologies were implemented. This has paved the way to the determination of the effects of component-level degradation on the system as a whole (G. Gorospe et al., 2017; G. E. Gorospe & Kulkarni, 2017). The development of new models and integration with previous models enables the simulation of a rotorcraft electric UAV propulsion system similar to that used in the Edge 540 electric UAV.

In Hogge et. al (Hogge et al., 2018), implementation of prognostic framework to batteries in electric powertrains was studied. In this work a distributed fault detection and isolation (FDI) framework is presented at the vehicle-level where different sub-systems like motors and ESCs interact with each other. In case of an UAS there could be four of such systems which need to be monitored for fault diagnosis at run time. We present implementation of the diagnostic framework to a generic quadcopter. It is assumed the four motors of the quadcopter are controlled by their respective ESCs and powered via a single LiPo battery pack. The diagnostic algorithm perform under the single-fault assumption, i.e., only one fault can be present in the system. We also assume faults to be abrupt and persistent faults.

Among the electric motor technologies available for propulsion systems, the permanent-magnet brushless direct-current (PDC) motors have seen increased use in fields beyond hobby aircraft communities where they are ubiquitous due to their availability and low cost (Gabriel, Meyer, & du Plessis, 2011). PDC motors do not use commutation and thus are more efficient, offer higher torque-to-weight ratio, and usually run quieter than brushed DC motors. An aircraft propulsion system typically consists of an energy storage device such as a lithium polymer battery (LiPo), electronic speed controllers (ESCs) to provide electric communication and frequency modulation based on control input, and the PDC motor which converts electrical energy to kinetic energy.

PDC machines are essentially synchronous machines with trapezoidal shaped induced emf. The ESC is responsible for monitoring the positions or modes and switching the current accordingly. Reduced performance of an ESC due to degradation can have negative consequences on both the battery and the motor leading to loss of thrust in the vehicle (Krishnan, 2009).

Previous work on fault diagnosis and health management for electric propulsion systems utilizing PDC motors has focused on open circuit winding faults and faults from malfunctioning transistor elements in power switching devices. Within transistor elements, both open-switch faults and low transistor base drive can lead to faulty conditions. To perform diagnostics on motor drive systems, in (Park, Kim, Ryu, & Hyun, 2006), the authors used a voltage sensor across the lower legs of the inverter to detect switch open-circuit faults, and fuses and switches to detect and mitigate switch short-circuit faults. Later, in (Park et al., 2011), the authors developed a diagnostic method by which the absolute value of the developed current on each leg of the inverter was monitored and summed, this sum was then compared with a threshold value. Below the threshold value, the likelihood of fault conditions was high. Awadallah et. al (Awadallah & Morcos, 2006) used a trained adaptive neuro-fuzzy inference system to not only detect the open switch fault but identify the faulty switch.

Other strategies for fault diagnosis and management have included the addition of supplementary phases (Gopalarathnam, Toliyat, & Moreira, 2000), fault management techniques, such as increasing current in healthy phases or extending conduction periods of healthy phases to make up for imbalances (Speed & Wallace, 1990), and methods for computing parameter changes expected during fault status (Moseler & Isermann, 2000).

Model-based diagnosis approaches can be broadly classified into centralized, decentralized, and distributed schemes, such as, (Gertler, 2017; Davis & Hamscher, 1988; Zhang, Polycarpou, & Parisini, 2002; Venkatasubramanian, Rengaswamy, Yin, & Kavuri, 2003). Centralized schemes, such as (Gertler, 2017), construct a single diagnoser from a global system model. Decentralized schemes, such as (Debouk, Lafortune, & Teneketzis, 2000), use a global system model but distribute the diagnosis computations among several local diagnosers. The local diagnosis decisions based on a subset of observations are communicated to other diagnosers, or to a central coordinator, which use the global model to generate globally consistent solutions.

Distributed diagnosis approaches use subsystem models and assume the global model is unknown (Kurien, Koutsoukos, & Zhao, 2002; Su & Wonham, 2005; Fabre, Benveniste, Haar, & Jard, 2005). Local diagnosers for each subsystem communicate their diagnosis results to each other to arrive at the global solution. Most decentralized and distributed diagnosis algorithms have been developed in the discrete-event framework (Kurien et al., 2002; Su & Wonham, 2005; Fabre et al., 2005; Baroni, Lamperti, Pogliano, & Zanella, 1999; Pencolé & Cordier, 2005). In (Debouk et al., 2000), the authors discuss three coordinated decentralized protocols for diagnosis that extend the centralized diagnosis method developed in (Sampath, Sengupta, Lafortune, Sinnamohideen, & Teneketzis, 1995). Each local diagnoser is built from the global system model and uses only a subset of observable events. Coordination is necessary in the first and second protocols to generate the correct diagnosis result, but the third protocol generates correct results without a coordinator. All three protocols, under certain assumptions, produce the same results as a centralized diagnoser. The approaches presented in (Baroni et al., 1999; Pencolé & Cordier, 2005) avoid coordination between local diagnosers by representing the system as a network of communicating finite state machines. First, the observable events for each subsystem are used to generate the individual subsystem diagnoses. Then, the subsystem diagnoses are merged to generate the global diagnosis result.

The offline approach presented in (Baroni et al., 1999) assumes all observable events are received in the same order that they were transmitted. The online approach described in (Pencolé & Cordier, 2005) achieves efficiency by avoiding merge operations for independent subsystems. Its incremen-

tal algorithm does not assume the ordering of observations is preserved. In (Kurien et al., 2002), the authors describe an approach where each local diagnoser generates a set of local diagnosis results, and then communicates with its neighbors to reduce the number of hypotheses. The graph of constraints between the fault hypotheses and the observations is partitioned to minimize communication between local diagnosers. A similar approach is presented in (Su & Wonham, 2005), where the partitioning is based on physical connections.

Our approach, designed for diagnosing faults in large continuous systems, differs from (Debouk et al., 2000; Kurien et al., 2002; Su & Wonham, 2005; Fabre et al., 2005; Baroni et al., 1999; Pencolé & Cordier, 2005). Abrupt parametric faults, i.e., a step change in a plant parameter value, produce transients in the system dynamics. Capturing these fault generated transient behaviors in a discrete-event model by quantizing the measurement or state-space can result in state explosion (Lunze, 2000). We adopt a different approach, where we use the continuous model to derive fault effects as qualitative magnitude and higher-order effects on individual measurements. This produces a compact model for online diagnosis. We use the global system model to design local diagnosers offline. At runtime, the local diagnosers operate independently to generate local diagnosis results that are globally correct. Our approach does not require a coordinator, and there is minimal or no exchange of information among the diagnosers. This is similar to the third protocol in (Debouk et al., 2000), and a failure in a local diagnoser does not affect the diagnosis capability of the other diagnosers. Therefore, our approach operates like other online distributed diagnosis schemes, such as, (Pencolé & Cordier, 2005).

The simulation experiments demonstrate how the distributed diagnosis algorithm correctly and efficiently diagnose faults in the rotorcraft's electric powertrain. In this work faults are injected in the motor and the ESCs of the rotorcraft. Developed fault detection and isolation frameworks identifies the respective faults in the subsystem based on observed sensor data.

### 3. SIMULATION CASE STUDY: ELECTRICAL PROPULSION SYSTEM

This paper is focused on detecting and isolating faults due to degradation observed in ESCs or motors in either of the four arms of the quadcopter under study. The supply voltage is set to 20 V DC which is sourced through a LiPo battery pack. The simulation model is build where in each of subsystems of the respective four arms are identical. The modeled electric propulsion system as seen in the Fig. 1 shows key components in a single arm which include a lithium-polymer battery as power source; an ESC consisting of a power conditioning circuit and gate driving circuit and a 3-phase power inverting circuit; and a PDC motor.

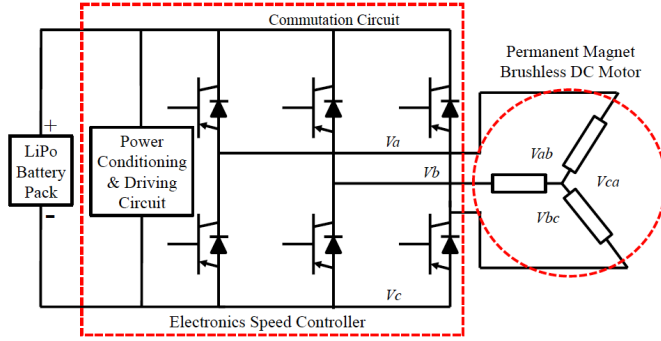


Figure 1. Schematic of an Electric UAV Propulsion System (Single Arm)

In the next sub-section, we discuss models developed for the ESC and PDC motor system respectively. Prognostics implementation on the battery system has been published in our earlier work (Hogge et al., 2018; Bole, Kulkarni, & Daigle, 2014; Bole et al., 2013). The battery model is not discussed in this work. The developed system models are then connected to form the entire electrical propulsion system for simulation in MATLAB. MATLAB Simulink 2017 is used for simulating the entire system as well as injecting faults. The simulation system is built on our earliest electric propulsion testbed (G. E. Gorospe & Kulkarni, 2017) for a fixed wing Edge 540 T mentioned earlier.

### 3.1. Electronic Speed Control Circuits Model

For the purposes of this research the ESC is modeled as an ideal power inverter employing sinusoidal pulse width modulation (SPWM) and half bridge drivers for each of three phases within a control block. Additionally, power switching devices are also modeled as ideal within the switching function block which represents the commutation functions of the ESC. This enables the study of switching faults, including open-circuit faults and short-circuit faults, and switching frequency faults such as shoot-through faults. This modeling scheme is representative of general ESC operation for PDC motors which involves battery input, pulse width modulation (PWM) input to control frequency, bridge drivers, and a semiconductor commutation circuit made up of switching transistors. Details of model development are discussed in (G. Gorospe et al., 2017).

Within the switching function block, F1, F2 and F3 are the PWM signals from the control block and are multiplied by the input voltage  $V$  (G. Gorospe et al., 2017). This amplifies the PWM signal that drives the 3 phase inverter. The output of the function is a 3-phase voltage,  $V_a$ ,  $V_b$ , and  $V_c$ , that is then connected to a wye motor function block in MATLAB given by Equation 1. F1, F2 and F3 are the outputs from the controlled block while  $v_{ab}$ ,  $v_{bc}$ ,  $v_{ca}$  are the winding voltages between respective phases.

$$\begin{bmatrix} 1 & -1 & 0 \\ 0 & 1 & -1 \\ -1 & 0 & 1 \end{bmatrix} V \begin{bmatrix} F1 \\ F2 \\ F3 \end{bmatrix} = \begin{bmatrix} v_{ab} \\ v_{bc} \\ v_{ca} \end{bmatrix} \quad (1)$$

The developed model is used to both simulate nominal as well as fault injected scenario operation of ESC. The data generated by this model in simulation can be directly compared with empirical data from laboratory testing.

### 3.2. Motor Dynamic Model

The dynamic model of the motor describes a three-phase brushless DC motor, with wye-connected stator windings and a permanent magnet as the rotor. This dynamic model only describes the mechanical device, and assumes that the electronic speed controller provides a given input to the three-phase terminals. Details of the developed model are discussed in (G. Gorospe et al., 2017).

If the three phase input voltage and back-emf trapezoids are given, then Equations 2, 3, and 4 can be used as the dynamic equations of the brushless DC motor (G. Gorospe et al., 2017).

$$\frac{d\omega_m}{dt} = \frac{1}{J}(-B\omega_m + (T_e(e, i) - T_l)), \quad (2)$$

where  $J$  is the inertia,  $B$  is the frictional coefficient, and  $T_l$  is the load torque on the rotor. Additionally, the rotor position,  $\theta_m$  is

$$\frac{d\theta_m}{dt} = \frac{p}{2}\omega_m, \quad (3)$$

where  $p$  is the number of poles, and

$$\frac{d}{dt} \begin{bmatrix} i_a \\ i_b \end{bmatrix} = -\frac{R_s}{L_M} \begin{bmatrix} i_a \\ i_b \end{bmatrix} + \frac{1}{L_M} \begin{bmatrix} 2 & 1 \\ 1 & 1 \end{bmatrix} \begin{bmatrix} v_{ab} \\ v_{bc} \end{bmatrix} - \frac{1}{L_M} \begin{bmatrix} 2 & -1 & -1 \\ 1 & 0 & -1 \end{bmatrix} \begin{bmatrix} e_a \\ e_b \\ e_c \end{bmatrix}. \quad (4)$$

## 4. THE DISTRIBUTED DIAGNOSTIC APPROACH

Model based diagnosis of complex systems enables their safe and efficient operation. Most model-based diagnosis schemes are centralized approaches that suffer from inherent disadvantages such as computational complexity, single point of failure, and scalability issues. Distributing the diagnosis task addresses these issues. This work is an application paper that discusses the implementation of our distributed health monitoring approach developed as part of earlier work (Roychoudhury, Biswas, & Koutsoukos, 2009).

Our distributed diagnosis scheme does not use a centralized coordinator, and each local diagnoser generates globally correct diagnosis results through local analysis, by only commu-

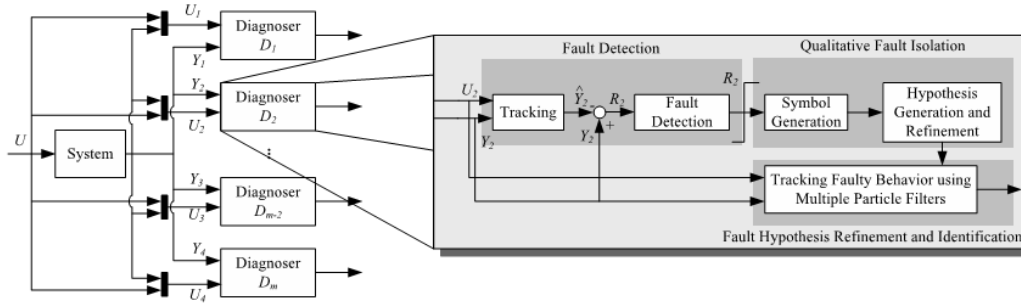


Figure 2. The distributed diagnosis architecture.

nicating a minimal number of measurements with other local diagnosers. The diagnoser design is based on the second algorithm presented in (Roychoudhury et al., 2009) that creates a partition structure and local diagnosers simultaneously. For each local diagnoser, separate particle filter (PF) based inference algorithms for fault detection, isolation, and identification are implemented. The quantitative diagnosis scheme is employed in combination with a qualitative fault isolation scheme to improve diagnosis efficiency. The schematic of our distributed diagnosis approach is shown in Fig. 2. Each local diagnoser performs three primary tasks: (i) fault detection, (ii) qualitative fault isolation (Qual-FI), and (iii) quantitative fault hypothesis refinement and identification (Quant-FHRI).

The fault hypothesis refinement and identification (FHRI) scheme is invoked when either the fault hypotheses set is refined to a pre-defined size,  $k$ , a design parameter, or a pre-specified  $s$  simulation time-steps have elapsed. For each fault hypothesis that remains when FHRI is initiated, a faulty system model is generated by extending the nominal model used by the local diagnoser to include the fault parameter as a stochastic variable. Again, a PF scheme for each fault model tracks the faulty observed behavior, taking as input the measurements from time  $t_d - \Delta^{max}$ , where  $\Delta^{max} \geq t_d - t_f$  is the maximum delay possible between the time of fault occurrence,  $t_f$ , and the time of fault detection,  $t_d$ . For each PF, a Z-test is used to determine if the deviation of a measurement estimated by the PF from the corresponding actual observation is statistically significant.

As more observations are obtained, ideally the PF using the correct fault model will eventually converge to the observed measurements, while the observations estimated using the incorrect fault models would gradually deviate from the observed measurements. We assume that the particles for the true fault model will converge to the observed measurements within  $s_d$  time steps of its invocation. Since the fault magnitude is included as a stochastic variable in every fault model, the magnitude of the true fault (i.e., the % bias) is considered to be that estimated by the PF for the true fault model.

## 5. EXPERIMENTS

The experiment is setup as a simulation for a quadcopter. Developed models are integrated in to form a single powertrain of the quadcopter powered by a single battery. Before discussing the experiment details we look into the different faults that could be occur in a electric power-train system. These have been listed based on the earlier work being done on respective systems (Daigle & Kulkarni, 2013; G. Gorospe et al., 2017). In this specific experiment we have integrated all the sub-systems together to form a single operational unit as would be the case on an electric UAV.

### 5.1. System Faults

As discussed the power-train system consists of three distinct subsystems that are susceptible to different faults modes and system degradation rates. Investigation into each of the systems leads to some of the prominent faults modes observed in the respective systems as discussed below.

- **LiPo Batteries:** Lithium corrosion, plating, electrolyte layer formation, and contact losses are examples of faults that batteries are susceptible to (Daigle & Kulkarni, 2013). These faults lead to an increase in internal resistance and impedance, as well as a decrease in charge capacity. Battery related faults are not discussed in this work.
- **Permanent Magnet Brushless DC Motors:** DC motors are susceptible to mechanical faults in the form of general motor or bearing wear, and electrical faults in the form of poor contacts and insulation deterioration (Abramov, Nikitin, Abramov, Sosnovichellasonovich, & Bozek, 2014; Awadallah & Morcos, 2002). Typically, changes in the vibration characteristics are caused by mechanical faults, and changes in the current draw characteristics are caused by electrical faults, but can also be caused by mechanical degradation. For example, bearing wear can result in increased friction, which would result in higher current draw to maintain the same output due to the increase in mechanical resistance. In addition due to high load usage the winding

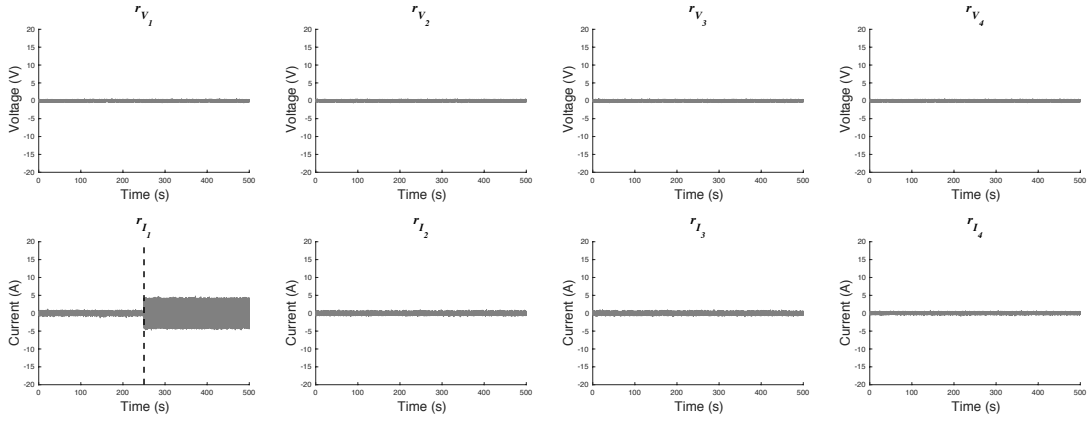


Figure 3. Insulation resistance change fault injected in Motor  $M_1$  at 250 s and detected at 250.03 s. Fault isolated at 255.03 s.

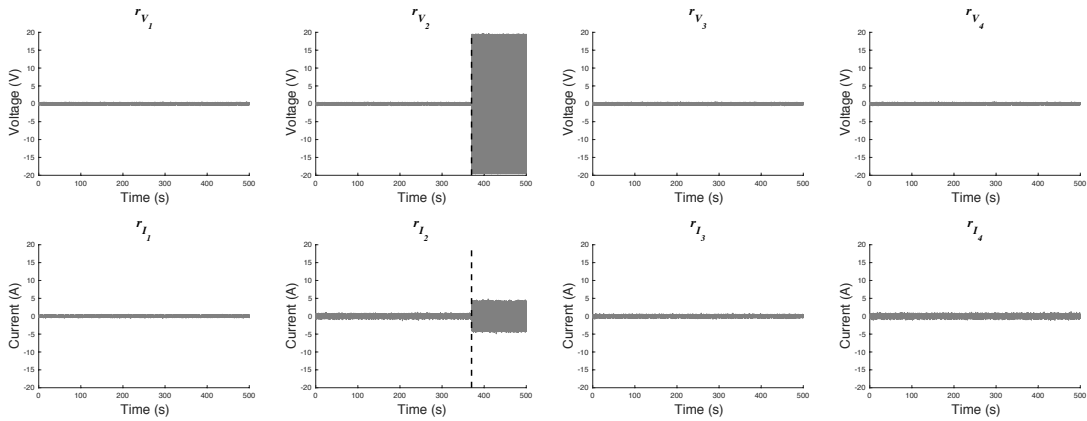


Figure 4. PWM frequency change fault injected in  $ESC_2$  at 370 s and fault detected and isolated at 370.02 s.

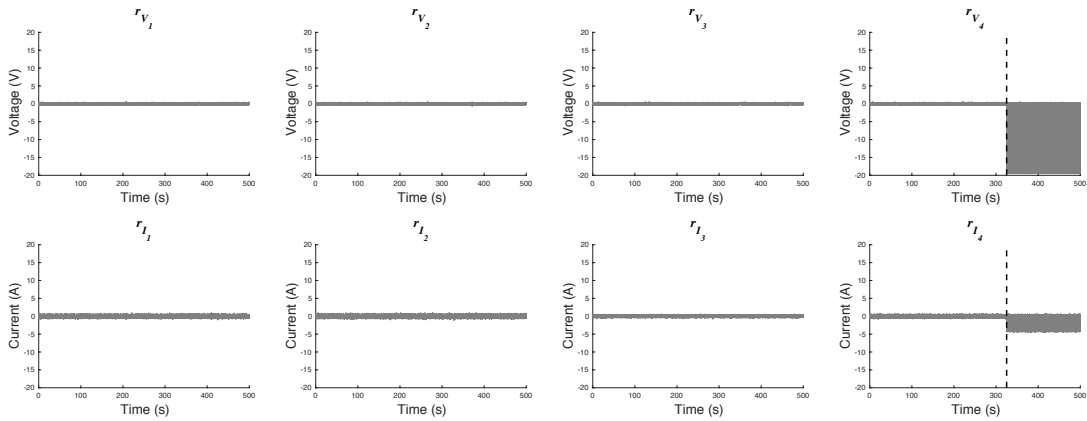


Figure 5. MOSFET struck open Fault injected in  $ESC_4$  at 325 s and fault detected and isolated at 325.03 s.

degrade over the period of time leading to change in insulation resistance. Winding faults can lead a short or open circuit condition. In this work we inject a winding

fault in one of the motor windings to observe change in the motor operation.

- **Electronics Speed Controllers:** ESCs are half bridge

rectifiers and most of the faults observed in them are due to switching circuits. Any faults in the conditioning circuit are not considered here. Faults are observed when the MOSFETs are not synchronized while operating, or when the switching circuit is malfunctioning (G. Gorospe et al., 2017). The first one results in a variable PWM control waveform, and the second one results in a non-operational voltage phase switching pair. Generally, a degraded ESC or an ESC operating under a faulty condition will draw more/less current than a healthy ESC when operating under similar environmental conditions and load.

## 5.2. Experimental Setup

As discussed in this work we have not incorporated the battery model and hence a constant source of 20V DC is used. For this study three faults are selected, two in the ESC system and one for the PDC motor. The faults are selected such that these could be replicated in a testbed environment later with updates being done to the current fixed wing testbed (G. E. Gorospe & Kulkarni, 2017).

The two selected faults in ESC system are: (1) change in the PWM control causes switching MOSFETs devices to operate at different frequencies and cause the output voltage and current to be out of sync leading to efficiency loss in motor operation and (2) MOSFET stuck open fault which may cause the half bridge rectifier circuit in the ESC incomplete leading to degradation in output rectified voltage.

A change in insulation resistance due to degradation is selected as a third fault which occurs in the motor windings. An increase in the motor winding insulation resistance leads to increased current draw leading to the batteries depleting at an increased discharge rate as well as heat being generated leading to increase in the winding temperature and hence overall motor-casing temperature. In this work we are not correlating the increase in current to temperature hence the sensor only measures voltage and current in the windings.

### 5.2.1. Problem

The systems are divided into input voltage through the batteries assumed constant and shared by all the four systems on each of the quadcopter arms. The sub-systems on each arm  $i$  consists of an ESC ( $ESC_i$ ) and a PDC motor ( $PDCM_i$ ). Under nominal operation the system runs for 500 s in total with voltage and current from each of the respective systems observed. When operating under faulty conditions each fault scenario in simulated individually.

Scenario  $M_1$  injects faults in one of the motor windings,  $E_{2A}$ ,  $E_{4B}$  inject PWM and MOSFET stuck fault in the second and fourth arm of the vehicle ESC system respectively. Voltages and currents from the respective systems are measured and compared against the nominal operation of the system. Ta-

ble 1 shown the fault signature matrix for electric powertrain. The parameters  $r_{I_i}$  and  $r_{V_i}$  are the residuals of current (I) and voltage (V), respectively between nominal and faulty scenario operations in the respective quadrotor sensor measurements.

As shown in Fig.2 the defined distributed diagnosers  $D_1$ ,  $D_2$ ,  $D_3$ , and  $D_4$  for the each of the four arms for the vehicle system consists of residuals  $r_{I_1}$ ,  $r_{V_1}$ ,  $r_{I_2}$ ,  $r_{V_2}$ ,  $r_{I_3}$ ,  $r_{V_3}$ ,  $r_{I_4}$ , and  $r_{V_4}$  respectively. The symbol generation approach described in (Roychoudhury et al., 2010) is used, which uses the Z-test for statistical fault detection and symbol generation. A window of samples is used to compute the mean, and thus can produce a delay that increases with window size. For the particular fault detector settings, we consider the bounded observation delay to be  $\Delta^{max} = 5$  s.

In the fault signature, a + indicates increase in deviation of the residual, a - indicates decrease in deviation of the residual on fault injection, and a 0 indicates no change. As discussed in section 2 only abrupt faults (denoted by a step change in the fault parameter) are injected.

Table 1. Fault Signature Matrix for Electric Powertrain.

Faults	$r_{I_1}$	$r_{V_1}$	$r_{I_2}$	$r_{V_2}$	$r_{I_3}$	$r_{V_3}$	$r_{I_4}$	$r_{V_4}$
$M_1$	+	0	0	0	0	0	0	0
$E_{1A}$	+	+	0	0	0	0	0	0
$E_{1B}$	-	-	0	0	0	0	0	0
$M_2$	0	0	+	0	0	0	0	0
$E_{2A}$	0	0	+	+	0	0	0	0
$E_{2B}$	0	0	-	-	0	0	0	0
$M_3$	0	0	0	0	+	0	0	0
$E_{3A}$	0	0	0	0	+	+	0	0
$E_{3B}$	0	0	0	0	-	-	0	0
$M_4$	0	0	0	0	0	0	+	0
$E_{4A}$	0	0	0	0	0	0	+	+
$E_{4B}$	0	0	0	0	0	0	-	-

## 5.3. Experimental Results

In this section, we demonstrate the approach through three example scenarios using the  $M_i$ ,  $E_{iA}$ ,  $E_{iB}$  fault scenarios. In all cases the system starts in the nominal state, and then faults are injected at different time points. The complete set of fault candidates are  $\{M_1, E_{1A}, E_{1B}, M_2, E_{2A}, E_{2B}, M_3, E_{3A}, E_{3B}, M_4, E_{4A}, E_{4B}\}$  as shown in table 1.

The symbol generation approach described in (Roychoudhury et al., 2010) is used, which uses the Z-test for statistical fault detection and symbol generation. A window of samples is used to compute the mean, and thus can produce a delay that increases with window size. For the particular fault detector settings, we consider the bounded observation delay to be  $\Delta^{max} = 5$  s.

**Example ( $M_1$  fault).** In this scenario, an increase in insulation resistance in the windings of motor  $M_1$  is injected at  $t_f = 250$  s. The measured and estimated values are shown in Fig. 3, which show that the behavior can be tracked through the mode changes during nominal operation. The residuals

are shown in Fig. 3. We first observe measurement  $I_1$  to increase at  $t_d = 250.03$  s, which can be caused by fault  $M_1$  or  $E_{1A}$  as can be seen from the fault signatures in Table 1. We then observe no other measurement change for 5 s, and we conclude the fault to be  $M_1$  at time 255.03 s.

**Example** ( $E_{2A}$  fault). In this scenario, a change in PWM frequency is injected in  $ESC_2$  at  $t_f = 370$  s. The measured and estimated values are shown in Fig. 4, which show that the behavior can be tracked through the mode changes during nominal operation. The residuals are shown in Fig. 4. We observe  $I_2$  as well as  $V_2$  to increase at  $t_d = 370.02$  s, which can be caused only by fault  $E_{2A}$  as can be seen from the fault signatures in Table 1. Hence, we conclude the fault to be  $E_{2A}$  at time 370.02 s.

**Example** ( $E_{4B}$  fault). In this scenario, an MOSFET stuck open fault is injected at  $t_f = 325$  s in the fourth arm ESC system of the quadcopter, i.e.,  $ESC_4$ . The measured and estimated values are shown in Fig. 5, which show that the behavior can be tracked through the mode changes during nominal operation. The residuals are shown in Fig. 5. We observe both measurements  $I_4$  and  $V_4$  decrease at  $t_d = 325.03$  s, which can be caused only due to  $E_{4B}$  as seen from fault signatures in Table 1). Hence, we conclude the fault to be  $E_{4B}$  at time 325.03 s.

## 6. CONCLUSION

The paper presented a distributed diagnosis approach for efficient diagnosis of faults in electric powertrain for a quadrotor vehicle. The implemented approach demonstrated that a distributed diagnoser can help diagnose faults without a coordinator and without any exchange of diagnostic results. Also, such distributed diagnosis scheme generates quick and efficient diagnosis results locally that are globally correct and requires very low computational cost.

This approach can be scaled to any rotorcraft with higher number of rotors (and hence, powertrains). Once the fault is accurately detected and isolated, one can implement a prognostics framework, such as those presented in (Daigle et al., 2015; Hogge et al., 2018) to systematically assess and estimate the health of the vehicle.

In the future, we would like to extend this work by combining the diagnostic and prognostic architecture to perform integrated system-level vehicle health management for safe operation. This integrated approach can also be extended to include additional system faults in the vehicle. Also, we would like to extend this work to diagnose multiple faults which are also discrete and incipient in nature.

## ACKNOWLEDGMENT

This work was funded by NASA System Wide Safety (SWS) project under the Airspace Operations and Safety (AOSP)

program within the NASA Aeronautics Research Mission Directorate (ARMD).

## REFERENCES

- Abramov, I. V., Nikitin, Y. R., Abramov, A. I., Sosnovichell- lasosnovich, E. V., & Bozek, P. (2014). Control and diagnostic model of brushless dc motor. In *Journal of electrical engineering*.
- Awadallah, M. A., & Morcos, M. M. (2002). Stator-winding fault diagnosis of pm brushless dc motor drives. In IEEE (Ed.), *Large engineering systems conference on power engineering*.
- Awadallah, M. A., & Morcos, M. M. (2006). Automatic diagnosis and location of open-switch fault in brushless dc motor drives using wavelets and neuro-fuzzy systems. *IEEE Transactions on Energy conversion*, 21(1), 104–111.
- Baroni, P., Lamperti, G., Pogliano, P., & Zanella, M. (1999). Diagnosis of large active systems. *Artificial Intelligence*, 110(1), 135–183.
- Bole, B., Kulkarni, C. S., & Daigle, M. (2014). Adaptation of an electrochemistry-based li-ion battery model to account for deterioration observed under randomized use. In *Annual conference of the prognostics and health management society*.
- Bole, B., Teubert, C., Chi, Q. C., Edward, H., Vazquez, S., Goebel, K., & Vachtsevanos, G. (2013). SIL/HIL replication of electric aircraft powertrain dynamics and inner-loop control for V&V of system health management routines. In *Annual conference of the prognostics and health management society*.
- Daigle, M., & Kulkarni, C. (2013, October). Electrochemistry-based battery modeling for prognostics. In *Annual conference of the prognostics and health management society 2013* (p. 249-261).
- Daigle, M., Sankararaman, S., & Kulkarni, C. (2015, March). Stochastic prediction of remaining driving time and distance for a planetary rover. In *2015 IEEE Aerospace Conference*.
- Davis, R., & Hamscher, W. (1988). Model-based reasoning: Troubleshooting. In *Exploring artificial intelligence* (pp. 297–346). Elsevier.
- Debouk, R., Lafortune, S., & Teneketzis, D. (2000). Coordinated decentralized protocols for failure diagnosis of discrete event systems. *Discrete Event Dynamic Sys-*

- tems*, 10(1-2), 33–86.
- Fabre, E., Benveniste, A., Haar, S., & Jard, C. (2005). Distributed monitoring of concurrent and asynchronous systems. *Discrete Event Dynamic Systems*, 15(1), 33–84.
- Gabriel, D. L., Meyer, J., & du Plessis, F. (2011). Brushless dc motor characterisation and selection for a fixed wing uav. In *Ieee africon*.
- Gertler, J. (2017). *Fault detection and diagnosis in engineering systems*. Routledge.
- Gopalathnam, T., Toliyat, H. A., & Moreira, J. C. (2000). Multi-phase fault-tolerant brushless dc motor drives. In *Industry applications conference, 2000. conference record of the 2000 IEEE* (Vol. 3, pp. 1683–1688).
- Gorospe, G., Kulkarni, C., & Hogge, E. (2017). A study of the degradation of electronic speed controllers for brushless dc motors. In *Asia pacific conference of the prognostics and health management society*.
- Gorospe, G. E., & Kulkarni, C. S. (2017). A novel uav electric propulsion testbed for diagnostics and prognostics. In *IEEE AUTOTESTCON*.
- Hogge, E., Bole, B., Vazquez, S., Kulkarni, C., Strom, T., Hill, B., . . . 8, C. Q. (2018). Verification of prognostic algorithms to predict remaining flying time for electric unmanned vehicles. In *International journal of prognostics and health management, issn 2153-2648, 2018 021*.
- Krishnan, R. (2009). *Permanent magnet synchronous and brushless dc motor drives*. CRC Press.
- Kulkarni, C. S., Celaya, J. R., Biswas, G., & Goebel, K. (2012). Towards a model-based prognostics methodology for electrolytic capacitors: A case study based on electrical overstress accelerated aging. *International Journal of Prognostics and Health Management*, 5(1), 16.
- Kurien, J., Koutsoukos, X., & Zhao, F. (2002). Distributed diagnosis of networked, embedded systems. In *13th international workshop on principles of diagnosis* (p. 179-188).
- Lunze, J. (2000). Diagnosis of quantized systems based on a timed discrete-event model. *IEEE Transactions on Systems, Man, and Cybernetics-Part A: Systems and Humans*, 30(3), 322–335.
- Moseler, O., & Isermann, R. (2000). Application of model-based fault detection to a brushless dc motor. *IEEE Transactions on industrial electronics*, 47(5), 1015–1020.
- Park, B.-G., Kim, T.-S., Ryu, J.-S., & Hyun, D.-S. (2006). Fault tolerant strategies for bldc motor drives under switch faults. In *Industry applications conference, 2006. 41st ias annual meeting. conference record of the 2006 IEEE* (Vol. 4, pp. 1637–1641).
- Park, B.-G., Lee, K.-J., Kim, R.-Y., Kim, T.-S., Ryu, J.-S., & Hyun, D.-S. (2011). Simple fault diagnosis based on operating characteristic of brushless direct-current motor drives. *IEEE Transactions on Industrial Electronics*, 58(5), 1586–1593.
- Pencolé, Y., & Cordier, M.-O. (2005). A formal framework for the decentralised diagnosis of large scale discrete event systems and its application to telecommunication networks. *Artificial Intelligence*, 164(1-2), 121–170.
- Roychoudhury, I., Biswas, G., & Koutsoukos, X. (2009). Designing distributed diagnosers for complex continuous systems. *IEEE Transactions on Automation Science and Engineering*, 6(2), 277–290.
- Roychoudhury, I., Biswas, G., & Koutsoukos, X. (2010). Distributed diagnosis in uncertain environments using dynamic bayesian networks. In *Control & automation (med), 2010 18th mediterranean conference on* (pp. 1531–1536).
- Sampath, M., Sengupta, R., Lafortune, S., Sinnamohideen, K., & Teneketzis, D. (1995). Diagnosability of discrete-event systems. *IEEE Transactions on automatic control*, 40(9), 1555–1575.
- Speed, R., & Wallace, A. K. (1990). Remedial strategies for brushless dc drive failures. *IEEE Transactions on industry Applications*, 26(2), 259–266.
- Su, R., & Wonham, W. M. (2005). Global and local consistencies in distributed fault diagnosis for discrete-event systems. *IEEE Transactions on Automatic Control*, 50(12), 1923–1935.
- Venkatasubramanian, V., Rengaswamy, R., Yin, K., & Kavuri, S. N. (2003). A review of process fault detection and diagnosis, part i: Quantitative model-based methods. *Computers and Chemical Engineering*, 27(3), 293-311.
- Zhang, X., Polycarpou, M. M., & Parisini, T. (2002). A robust detection and isolation scheme for abrupt and incipient faults in nonlinear systems. *IEEE transactions on automatic control*, 47(4), 576–593.